SIMULTANEOUS BLIND DECONVOLUTION AND PHASE RETRIEVAL WITH TENSOR ITERATIVE HARD THRESHOLDING

Shuang Li, Gongguo Tang, and Michael B. Wakin

Department of Electrical Engineering, Colorado School of Mines, Golden, CO, USA

ABSTRACT

Blind deconvolution and phase retrieval are both fundamental problems with a growing interest in signal processing and communications. In this work, we consider the task of simultaneous blind deconvolution and phase retrieval. We show that this non-linear problem can be reformulated as a low-rank tensor recovery problem and propose an algorithm named TIHT-BDPR to recover the unknown parameters. We include a series of numerical simulations to illustrate the effectiveness of our proposed algorithm.

Index Terms— Blind deconvolution, phase retrieval, low-rank tensor recovery, tensor IHT, HOSVD.

1. INTRODUCTION

Blind deconvolution and phase retrieval are problems of considerable interest in many applications including signal processing [1, 2] and image processing [3]. In image processing, blind deconvolution refers to the problem of recovering a sharp version of an image from its convolution with an unknown blur kernel [3]. Mathematically, the goal of blind deconvolution is to recover both x and g from their convolution $y = x \circledast g$. In phase retrieval problems, one aims to recover a complex signal x from the amplitude of its Fourier transform, i.e., $y = |\mathbf{F}x|^2$, where $\mathbf{F}$ is the DFT matrix.

Recently, low-rank tensor recovery problems have gained attention in many fields, such as hyperspectral image restoration [4], signal processing [5, 6], and video processing [7]. Nuclear norm minimization is a popular heuristic for rank minimization in low-rank matrix recovery problems and works well under suitable conditions on the measurement system [8,9]. Unfortunately, computation of the nuclear norm is NP-hard for high order tensors [10]. To develop a tractable method as an alternative to nuclear norm minimization, the authors in [11] extend the iterative hard thresholding (IHT) algorithm that is widely used in compressive sensing [12, 13] and low-rank matrix recovery [14] to the tensor setting and introduce the tensor IHT (TIHT) algorithm.

In this work, we address the problem of simultaneous blind deconvolution and phase retrieval (BDPR). In par-

ticular, we aim to recover a complex signal x and a real signal g from the convolution of $|\mathbf{F}x|^2$ and g, i.e., from $y = |\mathbf{F}x|^2 \circledast g$. This model may stem from phase imaging applications that employ partially coherent illumination (e.g. light bulbs, LEDs, and X-ray tubes) [15–17], rather than the traditional coherent (laser) illumination. In this situation, the forward model can be treated as the coherent situation with an extra convolution due to the source shape. We introduce a novel way to transform this non-linear problem into a low-rank tensor recovery problem. We also propose an algorithm named TIHT-BDPR by combining the TIHT algorithm and the higher order singular value decomposition (HOSVD) to solve this low-rank tensor recovery problem and recover the unknown parameters. Our numerical simulations show that the proposed algorithm can recover the low-rank tensor and the unknown parameters very well when provided with enough measurements. The authors in a recent work [18] address a similar problem of BDPR; however, both the signal models and proposed methods are different from ours. In particular, they relax their BDPR problem to a convex program with a lifted matrix recovery formulation.

The remainder of this work is organized as follows. In Section 2, we briefly review some basic concepts in tensor analysis. In Section 3, we define and transform the non-linear BDPR problem into a low-rank tensor recovery problem. We present the proposed TIHT-BDPR algorithm in Section 4 and illustrate its performance in Section 5. Finally, we conclude our work in Section 6.

2. PRELIMINARIES

A D-th order tensor $\mathcal{T} \in \mathbb{C}^{N_1 \times \cdots \times N_D}$ can be viewed as a high-dimensional extension of vectors and matrices. That is, vectors and matrices are special cases of tensors when D equals 1 and 2, respectively. Next, we briefly review some basic definitions and concepts used in tensor analysis [19, 20].

We define the *inner product* of two tensors $\mathcal{A}, \mathcal{B} \in \mathbb{C}^{N_1 \times \cdots \times N_D}$ as

$$\langle \mathcal{A}, \mathcal{B} \rangle \triangleq \sum_{n_1=1}^{N_1} \cdots \sum_{n_D=1}^{N_D} \mathcal{B}^*(n_1, \cdots, n_D)\mathcal{A}(n_1, \cdots, n_D),$$

where $\mathcal{A}(n_1, \cdots, n_D)$ is the $(n_1, \cdots, n_D)$-th entry of tensor

$\mathcal{A}$, and the same for $\mathcal{B}(n_1, \cdots, n_D)$.[1] The *Frobenius norm* of a tensor $\mathcal{A} \in \mathbb{C}^{N_1 \times \cdots \times N_D}$, induced by the above inner product, is given as

$$\|\mathcal{A}\|_F = \sqrt{\langle \mathcal{A}, \mathcal{A} \rangle}.$$

Let $\mathrm{rank}(\cdot)$ be an operator that computes the rank of a given matrix or tensor. We use the expression $[D]$ to denote the set $\{1, 2, \ldots, D\}$. Then, the *rank* of a D-th order tensor $\mathcal{T} \in \mathbb{C}^{N_1 \times \cdots \times N_D}$ is defined as a tuple $\boldsymbol{r} = (r_1, \cdots, r_D)$ with

$$r_d = \mathrm{rank}\left(\mathcal{T}^{\{d\}}\right), \quad d \in [D].$$

Here, matrix $\mathcal{T}^{\{d\}} \in \mathbb{C}^{N_d \times N_1 \cdots N_{d-1} N_{d+1} \cdots N_D}$ is the *mode-d matricization* or the *d-th unfolding*, which is defined as

$$\mathcal{T}^{\{d\}}(n_d; (n_l)_{l \in [D] \backslash d}) \triangleq \mathcal{T}(n_1, \cdots, n_D).$$

It can be seen that d and the indexes in $[D] \backslash d$ define the rows and columns of $\mathcal{T}^{\{d\}}$, respectively.

The HOSVD for a tensor $\mathcal{T} \in \mathbb{C}^{N_1 \times \cdots \times N_D}$ is a special case of the Tucker decomposition and is given as [21, 22]

$$\mathcal{T} = \mathcal{S} \times_1 \mathbf{U}^{(1)} \cdots \times_D \mathbf{U}^{(D)},$$

where $\mathcal{S} \in \mathbb{C}^{r_1 \times \cdots \times r_D}$ is the core tensor and $\mathbf{U}^{(d)} \in \mathbb{C}^{N_d \times r_d}$ denotes the basis with $r_d \leq N_d$. More details about the properties of $\mathcal{S}$ and $\mathbf{U}^{(d)}$ can be found in [11, 19, 20]. $\mathcal{S} \times_d \mathbf{U}^{(d)} \in \mathbb{C}^{r_1 \times \cdots \times r_{d-1} \times N_d \times r_{d+1} \times r_D}$ is the *mode-d product* of tensor $\mathcal{S}$ and a matrix $\mathbf{U}^{(d)}$, and is defined element-wise as

$$\begin{aligned}
&(\mathcal{S} \times_d \mathbf{U}^{(d)})(i_1, \cdots, i_{d-1}, n_d, i_{d+1}, \cdots, i_D) \\
&= \sum_{i_d=1}^{r_d} \mathcal{S}(i_1, \cdots, i_D) \mathbf{U}^{(d)}(n_d, i_d).
\end{aligned}$$

Let $\circ$ denote the tensor product. Note that

$$\mathcal{S} \times_1 \mathbf{U}^{(1)} \cdots \times_D \mathbf{U}^{(D)} = \mathcal{S} \mathbf{U}^{(1)} \circ \cdots \circ \mathbf{U}^{(D)} \quad (2.1)$$

if $r_d = 1$ for all $d \in [D]$, i.e., $\mathcal{S}$ is a scalar and $\mathbf{U}^{(d)}$ is a column vector.

3. PROBLEM FORMULATION

The BDPR problem considered in this work is motived by a real application in image processing. In particular, we consider phase imaging from a defocused intensity stack, which can be obtained by placing the detector at I different positions along the optical axis to take intensity images. With traditional coherent illumination, the i-th intensity image $\boldsymbol{y}_i \in \mathbb{R}^N$ can be written as[2]

$$\boldsymbol{y}_i = |\mathbf{F}(\boldsymbol{x} \odot \boldsymbol{g}_i)|^2, \quad i = 1, \ldots, I.$$

---

[1] Unless otherwise specified, we use the superscripts $\top$, H, and $*$ to denote transpose, conjugate transpose, and conjugate, respectively.

[2] Note that we formulate the two-dimensional image processing problem as a one-dimensional problem with vectorization. Then, we use one dimensional DFT and circular convolution in this work.

Here, $\mathbf{F} \in \mathbb{C}^{N \times N}$ is the DFT matrix with the (n_1, n_2)-th entry being $\mathbf{F}(n_1, n_2) = e^{-j2\pi(n_1-1)(n_2-1)/N}$, $\boldsymbol{g}_i \in \mathbb{C}^N$ is a Gaussian chirp phase mask that depends on the i-th position of the detector, and $\boldsymbol{x} \in \mathbb{C}^N$ is the complex field of the sample. We use $\odot$ to denote the elementwise (Hadamard) product. Rather than the traditional coherent illumination, we work on a more practical scenario in which partially coherent illumination is used. Partially coherent illumination, such as from light bulbs, LEDs, and X-ray tubes, is often unavoidable and even preferred for its improved light throughput, immunity to speckle noise, improved resolution (up to twice the coherent bandlimit) and better depth sectioning [15–17]. In this work, we seek to explicitly account for illumination coherence in our phase retrieval algorithms, allowing improved phase recovery in partially coherent systems with arbitrary light source shape. Using the Van Cittert-Zernike theorem [23], we propose to model coherence with a 2D function describing the source shape and treat the forward model as a coherent situation with an extra convolution due to the source shape:

$$\boldsymbol{y}_i = |\mathbf{F}(\boldsymbol{x} \odot \boldsymbol{g}_i)|^2 \circledast (\mathbf{P}_i \boldsymbol{s}), \quad i = 1, \ldots, I. \quad (3.1)$$

Here, $\circledast$ denotes circular convolution. The source shape $\boldsymbol{s} \in \mathbb{R}^N$ is an unknown, discretized source distribution function, and $\mathbf{P}_i \in \mathbb{R}^{N \times N}$ is a known linear operator that scales the source shape according to the detector position.

We assume that the unknown source shape $\boldsymbol{s}$ lives in a subspace spanned by the columns of a known matrix $\mathbf{B} \in \mathbb{R}^{N \times K}$ with $K \ll N$, namely, we can represent the source shape as $\boldsymbol{s} = \mathbf{B}\boldsymbol{h}$ with some coefficient vector $\boldsymbol{h} \in \mathbb{R}^K$. A recent work [24] shows an experimental validation of this with Gaussian bumps of different variances. Denote $\boldsymbol{b}_k \in \mathbb{R}^N$ as the k-th column of $\mathbf{B}$. Without loss of generality, we also assume that $\|\boldsymbol{h}\|_2 = 1$. Then, recovery of the source shape $\boldsymbol{s}$ is equivalent to the recovery of the unknown coefficient vector $\boldsymbol{h}$. In this work, our goal is to estimate both the source shape $\boldsymbol{s}$ and the complex sample field $\boldsymbol{x}$ from $\boldsymbol{y}_i$ in (3.1), which is a problem that combines blind deconvolution and phase retrieval.

Define an $N \times N$ circulant matrix as

$$\mathrm{circ}(\mathbf{P}_i \boldsymbol{b}_k) \triangleq \frac{1}{N} \mathbf{F}^H \triangle_{i,k} \mathbf{F}, \quad (3.2)$$

whose action corresponds to circular convolution with $\mathbf{P}_i \boldsymbol{b}_k$. Here, $\triangle_{i,k} \triangleq \mathrm{diag}(\mathbf{F} \mathbf{P}_i \boldsymbol{b}_k)$ is a diagonal matrix. Observe that

$$\begin{aligned}
\boldsymbol{y}_i &= |\mathbf{F}(\boldsymbol{x} \odot \boldsymbol{g}_i)|^2 \circledast (\mathbf{P}_i \boldsymbol{s}) = \sum_{k=1}^{K} \boldsymbol{h}(k) |\mathbf{F}(\boldsymbol{x} \odot \boldsymbol{g}_i)|^2 \circledast (\mathbf{P}_i \boldsymbol{b}_k) \\
&= \sum_{k=1}^{K} \boldsymbol{h}(k) \, \mathrm{circ}(\mathbf{P}_i \boldsymbol{b}_k) |\mathbf{F}(\boldsymbol{x} \odot \boldsymbol{g}_i)|^2 \\
&= \frac{1}{N} \sum_{k=1}^{K} \boldsymbol{h}(k) \mathbf{F}^H \triangle_{i,k} \mathbf{F} |\mathbf{F}(\boldsymbol{x} \odot \boldsymbol{g}_i)|^2,
\end{aligned}$$

2978

where the second equality follows from $\boldsymbol{s} = \sum_{k=1}^{K} \boldsymbol{h}(k)\boldsymbol{b}_k$ with $\boldsymbol{h}(k)$ being the k-th entry of $\boldsymbol{h} \in \mathbb{R}^K$ and the last equality follows by plugging (3.2). Denote $\boldsymbol{e}_n$ as the n-th column of an $N \times N$ identity matrix. Then, we can write the i-th intensity observation at pixel n, i.e., the n-th entry of $\boldsymbol{y}_i$, as

$$
\begin{aligned}
\boldsymbol{y}_i(n) &= \frac{1}{N}\sum_{k=1}^{K}\boldsymbol{h}(k)\boldsymbol{e}_n^H\mathbf{F}^H\triangle_{i,k}\mathbf{F}|\mathbf{F}(\boldsymbol{x}\odot\boldsymbol{g}_i)|^2 \\
&= \sum_{n_1=1}^{N}\sum_{n_2=1}^{N}\sum_{k=1}^{K}[\boldsymbol{x}(n_1)^*\boldsymbol{x}(n_2)\boldsymbol{h}(k)]\cdot\Big[\frac{1}{N}\big[\mathbf{F}(:,n_1)^H\boldsymbol{g}_i(n_1)^*\big] \\
&\quad \odot\big[\mathbf{F}(:,n_2)^\top\boldsymbol{g}_i(n_2)\big]\mathbf{F}^\top\mathrm{diag}(\mathbf{F}(:,n)^H)\mathbf{F}\mathbf{P}_i\boldsymbol{b}_k\big] \\
&= \langle \boldsymbol{x}^*\circ\boldsymbol{x}\circ\boldsymbol{h}, \mathcal{L}_{i,n}\rangle,
\end{aligned}
$$

where $\mathcal{L}_{i,n} \in \mathbb{C}^{N\times N\times K}$ is a sensing tensor with the (n_1, n_2, k)-th entry defined as

$$
\begin{aligned}
\mathcal{L}_{i,n}(n_1, n_2, k) &= \frac{1}{N}\big[\mathbf{F}(:,n_1)^\top\boldsymbol{g}_i(n_1)\big]\odot\big[\mathbf{F}(:,n_2)^H\boldsymbol{g}_i(n_2)^*\big] \\
&\quad \mathbf{F}^H\,\mathrm{diag}(\mathbf{F}(:,n))\mathbf{F}^*\mathbf{P}_i^*\boldsymbol{b}_k^*.
\end{aligned}
$$

(3.3)

Denote $\mathcal{L} : \mathbb{C}^{N\times N\times K} \to \mathbb{R}^{NI}$ as the composite linear operator used to obtain the measurements $\boldsymbol{y} \in \mathbb{R}^{NI}$, i.e., $\boldsymbol{y} = \mathcal{L}(\boldsymbol{x}^*\circ\boldsymbol{x}\circ\boldsymbol{h})$. In particular, we have $\boldsymbol{y} = [\boldsymbol{y}_1^\top \cdots \boldsymbol{y}_I^\top]^\top$ with

$$
\boldsymbol{y}_i(n) = \langle \boldsymbol{x}^*\circ\boldsymbol{x}\circ\boldsymbol{h}, \mathcal{L}_{i,n}\rangle,
$$

where $\mathcal{L}_{i,n} \in \mathbb{C}^{N\times N\times K}$ is a sensing tensor defined in (3.3). It follows from the observation (2.1) and definition of HOSVD that $\boldsymbol{x}^*\circ\boldsymbol{x}\circ\boldsymbol{h}$ is a rank-$\boldsymbol{r}_1$ tensor with $\boldsymbol{r}_1 = (1, 1, 1)$. Now, we can transform the non-linear BDPR problem (3.1) into a rank-$\boldsymbol{r}_1$ tensor recovery problem. Given the sensing tensor operator $\mathcal{L}$ and the linear measurements $\boldsymbol{y}$, we propose the following minimization program

$$
\{\widehat{\boldsymbol{x}}, \widehat{\boldsymbol{h}}\} = \arg\min_{\widetilde{\boldsymbol{x}},\widetilde{\boldsymbol{h}}} \frac{1}{2}\|\boldsymbol{y}-\mathcal{L}(\mathcal{T})\|_2^2 \text{ s.t. } \mathcal{T} = \widetilde{\boldsymbol{x}}^*\circ\widetilde{\boldsymbol{x}}\circ\widetilde{\boldsymbol{h}} \quad (3.4)
$$

to recover the rank-$\boldsymbol{r}_1$ tensor $\boldsymbol{x}^*\circ\boldsymbol{x}\circ\boldsymbol{h}$ as well as the original complex field sample $\boldsymbol{x}$ and the subspace coefficient $\boldsymbol{h}$.

As is known, the above minimization program is NP-hard in general. In matrix analysis, however, nuclear norm minimization is a popular heuristic of rank minimization problems and works well in low-rank matrix recovery under suitable conditions on the measurement system [8, 9]. Unfortunately, unlike matrices, computation of the nuclear norm is NP-hard for tensors with order $D \geq 3$ [10]. This motivates us to develop some other tractable method as an alternative.

4. THE PROPOSED TIHT-BDPR ALGORITHM

Inspired by the TIHT algorithm introduced in [11], we propose the TIHT-BDPR algorithm, which is summarized in Algorithm 1, by combining the TIHT algorithm and the

---

Algorithm 1 TIHT-BDPR

Input: $\mathcal{L}, \boldsymbol{y}, M, \{\mu_m\}_{m=1}^M, N, K$.
Output: $\widehat{\boldsymbol{x}}, \widehat{\boldsymbol{h}}$.
Initialize: $\mathcal{T}^0 = \boldsymbol{0}$.
for $m = 1, 2, \ldots, M$ **do**
    Compute $\widetilde{\mathcal{T}}^m = \mathcal{T}^{m-1} + \mu_m\mathcal{L}^*(\boldsymbol{y} - \mathcal{L}(\mathcal{T}^{m-1}))$.
    Compute $\mathcal{T}^m = \mathcal{P}_{\boldsymbol{r}_1}(\widetilde{\mathcal{T}}^m)$.
end for
Perform truncated HOSVD on $\widehat{\mathcal{T}} = \mathcal{T}^M$:

$$
\{\mathbf{U}^{(1)}, \mathbf{U}^{(2)}, \mathbf{U}^{(3)}, \mathcal{S}\} = \mathrm{HOSVD}(\widehat{\mathcal{T}}, \boldsymbol{r}_1).
$$

if $\mathbf{U}^{(1)} \neq \mathbf{U}^{(2)^*}$ **then** $\mathbf{U}^{(1)} = -\mathbf{U}^{(1)}, \mathbf{U}^{(3)} = -\mathbf{U}^{(3)}$
end if
Compute $\widehat{\boldsymbol{x}} = \sqrt{\mathcal{S}}\mathbf{U}^{(2)}$, and $\widehat{\boldsymbol{h}} = \mathbf{U}^{(3)}$.

HOSVD. We divide the process of solving program (3.4) into two parts: (i) finding a rank-$\boldsymbol{r}_1$ tensor $\widehat{\mathcal{T}}$ with TIHT by solving the following minimization problem

$$
\widehat{\mathcal{T}} = \arg\min_{\mathcal{T}} \frac{1}{2}\|\boldsymbol{y} - \mathcal{L}(\mathcal{T})\|_2^2 \quad \text{s.t. } \mathrm{rank}(\mathcal{T}) = \boldsymbol{r}_1,
$$

and (ii) estimating $\{\boldsymbol{x}, \boldsymbol{h}\}$ by computing the truncated HOSVD of $\widehat{\mathcal{T}}$.[3]

In the first part of Algorithm 1, $\mathcal{L}^* \in \mathbb{R}^{NI} \to \mathbb{C}^{N\times N\times K}$ is the corresponding adjoint operator of $\mathcal{L}$. We use μ_m to denote the step size parameter at the m-th iteration. $\mathcal{P}_{\boldsymbol{r}_1}$ is an operator that computes a rank-$\boldsymbol{r}_1$ approximation of a given tensor via the HOSVD. In the second part, based on the conjugate symmetry property of the first two components in the rank-$\boldsymbol{r}_1$ tensor $\widehat{\mathcal{T}}$ and the sign ambiguity that exists in a tensor decomposition, we have added an extra step after the HOSVD to remove this sign ambiguity. As we fix $\boldsymbol{r}_1 = (1, 1, 1)$, the HOSVD returned core tensor $\mathcal{S}$ becomes a scalar while the bases $\mathbf{U}^{(1)}, \mathbf{U}^{(2)}, \mathbf{U}^{(3)}$ are all vectors with unit ℓ_2-norm.

Fixing the index k, note that $\mathcal{L}_{i,n}(:, :, k) \in \mathbb{C}^{N\times N}$ defined in (3.3) is a Hermitian matrix. This Hermitian structure of the sensing tensors preserves the symmetry property of $\widehat{\mathcal{T}}$, i.e., $\mathbf{U}^{(1)} = \mathbf{U}^{(2)^*}$, up to a sign ambiguity if we start the TIHT-BDPR algorithm with zero initialization.

5. NUMERICAL SIMULATIONS

In this section, we illustrate the effectiveness of the proposed TIHT-BDPR algorithm with some numerical experiments. We set the parameters $N = 25$ and $K = 2$. Then, we create the complex field sample $\boldsymbol{x} \in \mathbb{C}^N$ as a complex Gaussian vector with entries satisfying $\mathcal{CN}(0, 1)$. The subspace coefficient vector $\boldsymbol{h} \in \mathbb{R}^K$ is generated as a real Gaussian vector with entries satisfying $\mathcal{N}(0, 1)$. The subspace matrix

---

[3]In this work, we use a Matlab toolbox named Tensorlab to compute the truncated HOSVD [25].

$\mathbf{B} \in \mathbb{R}^{N \times K}$ is also generated as a real Gaussian matrix with entries satisfying $\mathcal{N}(0, 1)$. To simplify the simulation, we use a set of length N complex Gaussian vectors $\boldsymbol{g}_i \in \mathbb{C}^N$ with entries following $\mathcal{CN}(0, 1)$ instead of the Gaussian chirp phase mask. The linear operator $\mathbf{P}_i \in \mathbb{R}^{N \times N}$ is also created as a real Gaussian matrix with entries satisfying $\mathcal{N}(0, 1)$.[4] Then, the measurements $\boldsymbol{y}$ and sensing tensors $\mathcal{L}_{i,n}$ are generated according to (3.1) and (3.3), respectively.

To implement the proposed TIHT-BDPR algorithm, we set the step size $\mu_m = 1$ for all m. We start with zero initialization and set the maximal number of iterations as $M = 5 \times 10^4$. The simulation results with $I = 5$ and $I = 20$ are shown in Figs. 1 and 2, respectively. To better illustrate the results, we reshape the absolute value and global phase ambiguity of $\boldsymbol{x}$ and $\widehat{\boldsymbol{x}}$ to a 5×5 matrix. Note that there is a phase ambiguity problem in phase retrieval, therefore, we can only recovery the phase of $\boldsymbol{x}$ up to a global phase ambiguity. In particular, we view the estimated phase $\angle \widehat{\boldsymbol{x}}$ as a perfect recovery as long as the entries in vector $e^{j\angle \boldsymbol{x}}/e^{j\angle \widehat{\boldsymbol{x}}}$ are equal. Denote $\mathcal{T}^\star = \boldsymbol{x}^* \circ \boldsymbol{x} \circ \boldsymbol{h}$, $\boldsymbol{x}$, and $\boldsymbol{h}$ as the true tensor, complex field sample, and subspace coefficient vector, respectively. Let $\widehat{\mathcal{T}}$, $\widehat{\boldsymbol{x}}$, and $\widehat{\boldsymbol{h}}$ denote the recovered tensor, complex field sample, and subspace coefficient vector, respectively. We define the relative recovery error between tensors, absolute value of complex field sample, and subspace coefficient vector as

$$\Delta_{\mathcal{T}} \triangleq \frac{\|\mathcal{T}^\star - \widehat{\mathcal{T}}\|_F}{\|\mathcal{T}^\star\|_F}, \ \Delta_{|\boldsymbol{x}|} \triangleq \frac{\||\boldsymbol{x}| - |\widehat{\boldsymbol{x}}|\|_2}{\|\boldsymbol{x}\|_2}, \ \Delta_{\boldsymbol{h}} \triangleq \|\boldsymbol{h} - \widehat{\boldsymbol{h}}\|.$$

Note that $\|\boldsymbol{h}\|_2 = 1$, so the relative recovery error between the true and recovered subspace coefficient vector is $\|\boldsymbol{h} - \widehat{\boldsymbol{h}}\|_2$. We present the relative recovery error for $I = 3, 5$, and 20 in Table 1. It can be seen that the TIHT-BDPR algorithm can provide accurate estimation of the complex field sample $\boldsymbol{x}$, subspace coefficient vector $\boldsymbol{h}$, and the rank-r_1 tensor, as long as the number of detector positions I is large enough. The bottom right plots (d) in Figs. 1 and 2 also indicate a linear convergence of our proposed algorithm.

6. CONCLUSION

In this paper, we work on the problem of simultaneous blind deconvolution and phase retrieval. In particular, we transform this non-linear problem into a linear inverse problem, namely, a rank-$(1, 1, 1)$ tensor recovery problem. Meanwhile, we propose an algorithm named TIHT-BDPR to solve this rank-$(1, 1, 1)$ tensor recovery problem. Numerical simulations indicate that the proposed algorithm works very well. We leave the convergence analysis and robust performance analysis on noisy measurements for future work.

---

[4]Note that we have used several random assumptions here, which may not be satisfied in the imaging model that motivated our problem. However, these assumptions can extremely simplify our simulations and provide us a sense of the overall sample complexity.
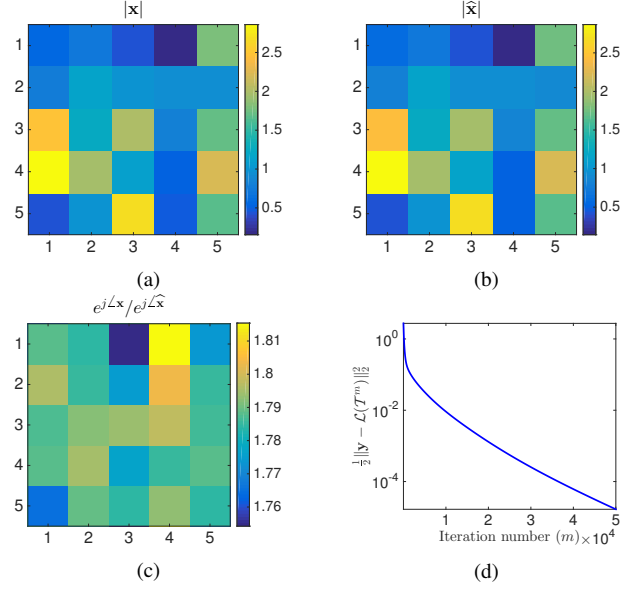
Fig. 1: $I = 5$: (a) the absolute value of the true $\boldsymbol{x}$, (b) the absolute value of the estimated $\widehat{\boldsymbol{x}}$, (c) the global phase ambiguity, (d) the cost function $\frac{1}{2}\|\boldsymbol{y} - \mathcal{L}(\mathcal{T}^m)\|_2^2$ at each iteration.
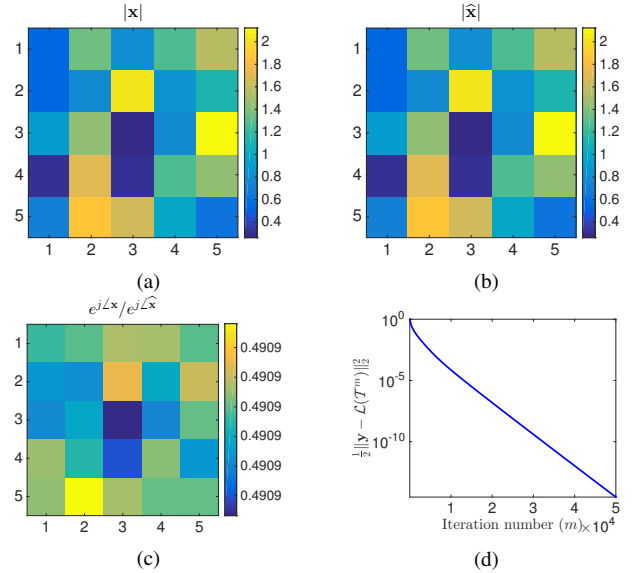
Fig. 2: $I = 20$: (a) the absolute value of the true $\boldsymbol{x}$, (b) the absolute value of the estimated $\widehat{\boldsymbol{x}}$, (c) the global phase ambiguity, (d) the cost function $\frac{1}{2}\|\boldsymbol{y} - \mathcal{L}(\mathcal{T}^m)\|_2^2$ at each iteration.

	$\Delta_{\mathcal{T}}$	$\Delta_{|\boldsymbol{x}|}$	$\Delta_{\boldsymbol{h}}$
$I = 3$	1.2244	0.4818	0.0386
$I = 5$	0.0138	0.0073	6.5894×10^{-4}
$I = 20$	1.2511×10^{-7}	6.0466×10^{-8}	4.9409×10^{-9}

Table 1: Relative recovery error for $I = 3, 5$, and 20.

2980

7. REFERENCES

[1] E. J. Candès, Y. C. Eldar, T. Strohmer, and V. Voroninski, "Phase retrieval via matrix completion," *SIAM Review*, vol. 57, no. 2, pp. 225–251, 2015.

[2] Y. Chi, "Guaranteed blind sparse spikes deconvolution via lifting and convex optimization.," *IEEE Journal of Selected Topics in Signal Processing*, vol. 10, no. 4, pp. 782–794, 2016.

[3] D. Kundur and D. Hatzinakos, "Blind image deconvolution," *IEEE Signal Processing Magazine*, vol. 13, no. 3, pp. 43–64, 1996.

[4] H. Fan, Y. Chen, Y. Guo, H. Zhang, and G. Kuang, "Hyperspectral image restoration using low-rank tensor recovery," *IEEE Journal of Selected Topics in Applied Earth Observations and Remote Sensing*, vol. 10, no. 10, pp. 4589–4604, 2017.

[5] Q. Li, A. Prater, L. Shen, and G. Tang, "Overcomplete tensor decomposition via convex optimization," in *2015 IEEE 6th International Workshop on Computational Advances in Multi-Sensor Adaptive Processing (CAMSAP)*, pp. 53–56, 2015.

[6] Q. Li, S. Li, H. Mansour, M. B. Wakin, D. Yang, and Z. Zhu, "Jazz: A companion to music for frequency estimation with missing data," in *2017 IEEE International Conference on Acoustics, Speech and Signal Processing (ICASSP)*, pp. 3236–3240, 2017.

[7] J. A. Bengua, H. N. Phien, H. D. Tuan, and M. N. Do, "Efficient tensor completion for color image and video recovery: Low-rank tensor train," *IEEE Transactions on Image Processing*, vol. 26, no. 5, pp. 2466–2479, 2017.

[8] E. J. Candès and B. Recht, "Exact matrix completion via convex optimization," *Foundations of Computational Mathematics*, vol. 9, no. 6, pp. 717–772, 2009.

[9] S. Li, H. Mansour, and M. B. Wakin, "An optimization view of music and its extension to missing data," *arXiv preprint arXiv:1806.03511*, 2018.

[10] C. J. Hillar and L.-H. Lim, "Most tensor problems are np-hard," *Journal of the ACM (JACM)*, vol. 60, no. 6, p. 45, 2013.

[11] H. Rauhut, R. Schneider, and Z. Stojanac, "Low rank tensor recovery via iterative hard thresholding," *Linear Algebra and its Applications*, vol. 523, pp. 220–262, 2017.

[12] T. Blumensath and M. E. Davies, "Iterative hard thresholding for compressed sensing," *Applied and Computational Harmonic Analysis*, vol. 27, no. 3, pp. 265–274, 2009.

[13] J. Qin, S. Li, D. Needell, A. Ma, R. Grotheer, C. Huang, and N. Durgin, "Stochastic greedy algorithms for multiple measurement vectors," *arXiv preprint arXiv:1711.01521*, 2017.

[14] J. Tanner and K. Wei, "Normalized iterative hard thresholding for matrix completion," *SIAM Journal on Scientific Computing*, vol. 35, no. 5, pp. S104–S125, 2013.

[15] E. Barone-Nugent, A. Barty, and K. Nugent, "Quantitative phase-amplitude microscopy i: optical microscopy," *Journal of Microscopy*, vol. 206, no. 3, pp. 194–203, 2002.

[16] F. Pfeiffer, T. Weitkamp, O. Bunk, and C. David, "Phase retrieval and differential phase-contrast imaging with low-brilliance x-ray sources," *Nature Physics*, vol. 2, no. 4, pp. 258–261, 2006.

[17] L. Reimer, R. Rennekamp, I. Fromm, and M. Langenfeld, "Contrast in the electron spectroscopic imaging mode of a tem: Iv. thick specimens imaged by the most-probable energy loss," *Journal of Microscopy*, vol. 162, no. 1, pp. 3–14, 1991.

[18] A. Ahmed, A. Aghasi, and P. Hand, "Blind deconvolutional phase retrieval via convex programming," *arXiv preprint arXiv:1806.08091*, 2018.

[19] I. S. Sokolnikoff, *Tensor analysis: Theory and applications*. Wiley, 1951.

[20] X.-D. Zhang, *Matrix analysis and applications*. Cambridge University Press, 2017.

[21] L. R. Tucker, "Implications of factor analysis of three-way matrices for measurement of change," *Problems in Measuring Change, University of Wisconsin Press Madison*, vol. 15, pp. 122–137, 1963.

[22] L. R. Tucker, "The extension of factor analysis to three-dimensional matrices," *Contributions to Mathematical Psychology, Holt, Rinehart and Winston, New York*, pp. 110–127, 1964.

[23] M. Born and E. Wolf, *Principles of optics: electromagnetic theory of propagation, interference and diffraction of light*. Elsevier, 2013.

[24] D. Yang, G. Tang, and M. B. Wakin, "Super-resolution of complex exponentials from modulations with unknown waveforms," *IEEE Transactions on Information Theory*, vol. 62, no. 10, pp. 5809–5830, 2016.

[25] N. Vervliet, O. Debals, L. Sorber, M. Van Barel, and L. De Lathauwer, "Tensorlab 3.0," *available online, URL: www.tensorlab.net*, 2016.